Activation measurements in support of the 14 MeV neutron calibration of JET neutron monitors

Activation measurements in support of the 14 MeV neutron calibration of JET neutron monitors

S. Jednorog[a], E. Laszynska[a], P. Batistoni[b], B. Bienkowska[a], A. Cufar[c], Z. Ghani[d], L. Giacomelli[e], A. Klix[f], S. Loreti[b], K. Mikszuta[a], L. Packer[d], A. Peacock[d], M. Pillon[b], S. Popovichev[d], M. Rebai[g], D. Rigamonti[g], N. Roberts[h], M. Tardocchi[e], D. Thomas[h] and JET Contributors*

[a] Institute of Plasma Physics and Laser Microfusion, Hery 23, 01-497 Warsaw, Poland
[b] ENEA, Department of Fusion and Nuclear Safety Technology, I-00044 Frascati (Rome) Italy
[c] Jozef Stefan Institute, Jamova cesta 39, 1000, Ljubljana, Slovenia
[d] Culham Science Centre, Abingdon, Oxon, OX14 3DB, United Kingdom
[e] Istituto di Fisica del Plasma CNR, Milano, Italy
[f] Karlsruhe Institute of Technology, 76344 Eggenstein-Leopoldshafen, Karlsruhe, Germany
[g] Dipartimento di Fisica Università degli Studi di Milano-Bicocca, Milano, Italy
[h] National Physics Laboratory, TW11 OLW Teddington, United Kingdom
[*] See the author list of "Overview of the JET results in support to ITER" by X. Litaudon et al. to be published in Nuclear Fusion Special issue: overview and summary reports from the 26th Fusion Energy Conference (Kyoto, Japan, 17-22 October 2016)

Corresponding author: katarzyna.mikszuta@ifpilm.pl

Abstract

In preparation for the upcoming deuterium-tritium campaign at the JET tokamak, the ex-vessel fission chamber neutron diagnostics and the neutron activation system will be calibrated in absolute terms at 14 MeV neutron energy, to a required accuracy of less than 10 %. Two identical DT neutron generators were chosen as the calibration sources, both of which were fully calibrated and characterised at the UK's National Physical Laboratory (NPL). The neutron activation method was adopted as a complementary method for the purpose of determining the absolute value of the neutron yield from the neutron generators and to provide a means of cross check for the active detection methods being employed. The relative neutron intensity was measured utilising two Single Crystal Diamond Detectors with less than 1 % uncertainty. The work being presented here shows the derivation of the neutron emission rate from the neutron generators based upon experimental activation foil measurements. The reaction products chosen for the 14-MeV neutron measurements included the standard activation products: ^{92m}Nb, ^{24}Na, ^{56}Mn and ^{27}Mg; all of which were measured with an uncertainty less than 9%. The neutron generator yields were derived from the mean emission rate of the four different activation reactions, resulting in neutron yields of approximately $2.4 \cdot 10^{8}$ $n \cdot s^{-1}$ for the first neutron generator, with a standard deviation of 2.4-5.3 %, before it dropped permanently, during the experimental campaign, by 20% . For the same parameter settings, the second neutron generators mean neutron emission rate was calculated to be approximately $2.2 \cdot 10^{8}$ $n \cdot s^{-1}$ with a standard deviation in the range of 3.2-6.0 %.

Keywords: JET D-T campaign, neutron yield calibration, neutron generator, activation technique

1. Introduction

The absolute measurement of neutron yield (Y_n), in a fusion device, is needed to provide the fusion power output along with other plasma parameters, such as the ion temperature and density.

The system of neutron yield monitors used to monitor the Joint European Torus (JET) consists of $^{235}U/^{238}U$ fission chambers (KN1), located outside the tokamak, and an internal, in-vessel, activation system (KN2). An absolute calibration of both KN1 $^{235}U/^{238}U$ fission chambers and KN2 was performed in 2013, using a ^{252}Cf spontaneous-fission source, having a mean energy of 2.1 MeV and a source strength of $2.4 \cdot 10^8$ n·s^{-1}. JET operating in deuterium (D) mode produces 2.5-MeV neutrons by the (d,d) fusion reaction, the ^{252}Cf neutron energy spectrum is sufficiently similar to the (d,d) fusion energy distribution; that it serves as an adequate calibration measure for neutrons of such similar energies. Additionally, MCNP [1] calculations were used to determine the correctional factors arising from the differences in the neutron spectrum from that of a pure D plasma and other geometrically dependant calibration factors [2].

The neutron source (NS) was placed at different points inside the vacuum vessel, from which neutron induced activation and fission chamber pulses were recorded by KN1 and KN2 systems, respectively. In KN2 the $^{115}In(n,n')^{115m}In$ nuclear reaction is used as the monitoring reaction in D operations. The cross section has a maximum at an energy of 2.7 MeV, which is useful for measuring the 2.5 MeV neutrons released during deuterium fusion, and has a threshold of approximately 0.4 MeV. The moderated $^{235}U/^{238}U$ fission chambers can measure a broad energy range of neutrons and have a relatively flat response over these energies. During the 2013 calibration campaign, both KN1 and KN2 were calibrated with a total uncertainty of approximately ±10 %; these results were successfully verified during the following D campaign [S. Popovichev, private communication].

A new Deuterium-Tritium Experimental Campaign (DTE2) on the JET tokamak is planned in the near future [3]; in which up to $1.7 \cdot 10^{21}$, 14.1 MeV neutrons will be produced, a new calibration of JET monitoring systems for higher energy neutrons therefore is required.

JET calibration, at 14.1 MeV neutron energy, requires the use of a different set of nuclear reactions, with higher energy thresholds, and at the same time, sufficiently high cross section and convenient decay times of the reaction products. Moreover, the tokamak transparency to neutrons alters as the neutron energy increases from 2.5 MeV to 14.1 MeV, thus, causing a change in the response of the ^{235}U fission chambers. To accurately determine calibration coefficients, it is therefore necessary to conduct a JET neutron diagnostic calibration with a NS that emits 14.1-MeV neutrons from a (d,t) reaction. The 14-MeV calibration will be based on the procedures and experience gained during the 2.5-MeV calibration [2]. The experience gained during the 14.1-MeV calibration of JET neutron diagnostics will serve as a good methodology when calibrations are carried out on ITER, which is currently under construction in Cadarache, France.

The ING-17 neutron generator (NG) [4] manufactured by the All-Russia Research Institute of Automatics (VNIIA) Moscow, Russian Federation [5] was chosen as the neutron source for neutron calibration of JET. It has a nominal yield of approximately $2 \cdot 10^8$ n·s^{-1}. The NG comprises of an accelerated beam consisting of deuterium and tritium ions and of ionized molecules, striking a target made of tritium and deuterium, in an approximate 50/50 % ratio, implanted onto titanium. The yield of neutrons emitted is strongly dependent upon the beam acceleration voltage.

In order for the NG to be used as a calibration source, the yield must be known with a high accuracy, possibly better than ±5 %. The emitted neutron energy spectrum characteristics must also be known. The NG emission characteristics were measured during two experimental campaigns at the UK National Physical Laboratory (NPL) by the NPL Neutron Metrology Group, using their low-scatter cell neutron facility. Two nominally identical NGs (NG1 and NG2) were examined. They were mounted in the centre of the large hall (see fig. 1), where the conditions support the low scatter requirements. The emission rates and energy spectrums of both NGs were measured by "characterization" neutron detectors: an absolutely calibrated De Pangher long counter; an absolutely calibrated NPL long counter; two Single Crystal Diamond Detector (SDD) -neutron spectrometer; a NE-213 scintillator based neutron spectrometer [6] and activation foils. From these measurements, the two NGs total neutron yield in 4π can be derived.

Fig. 1 *Experimental hall inside the Chadwick facility. The NG is located in the centre of the hall. The two long counters and the NE-213 scintillator are situated above the red rails in the centre of the above image.*

The NG emission rate and energy spectrum vary over the course of a single run [7]. It is therefore necessary to monitor the varying yield during the whole calibration process. In order to do this, the NG was equipped with "monitoring" detectors, both active and passive. These comprised: i) a SDD and a Silicon diode in the first campaign, two SDD in the second campaign, and ii) a set of 12 activation foils, all located in well-defined, stable positions relative to the neutron generator target; where the neutrons are produced. These monitoring detectors were attached to the NGs by means of a mechanical support (see fig. 2).

The SDDs measurements, combined with the measurements by the absolutely calibrated long counter measurements carried out at NPL, provide the absolute time resolved emission rate from the NG. The activation foils provide a complementary and independent measurement of the absolute neutron emission rate ($n \cdot s^{-1}$) for a given exposure period. This paper focuses on the measurement and analyses of the monitoring activation foils,

and on the comparison with the active monitoring detectors. The uncertainty of the derived absolute neutron emission rate of the NGs is also discussed.

2. Experiment set up

A set of monitoring activation foils were attached to a custom made holder and mounted on the NG mechanical support (fig. 2). The holder was designed to allow for retrieval by the JET remote handling system during the in-vessel calibration of the JET tokamak. The mechanical support used in the second campaign was a slight variation on the one used in the first campaign; which was modified to improve the positioning of monitoring detectors with respect to the NG target. Both the SDDs and the activation foils will be used during the in vessel calibration at JET, which will implement the same mechanical support and positioning system used in the second NPL campaign.

The NG irradiation schedule at NPL consisted of a series of 20-minute irradiations followed by 10 minutes of NG cooling. During the cooling periods, the positions of the non-attached neutron diagnostics were changed and other necessary anisotropy measurements were carried out. The daily operational cycle consisted of 11-13 irradiations, except for the first day, where only two irradiations were completed. The monitoring activation foils were normally removed after the ninth irradiation cycle; to allow the gamma spectrometry measurements to be started at a practical time.

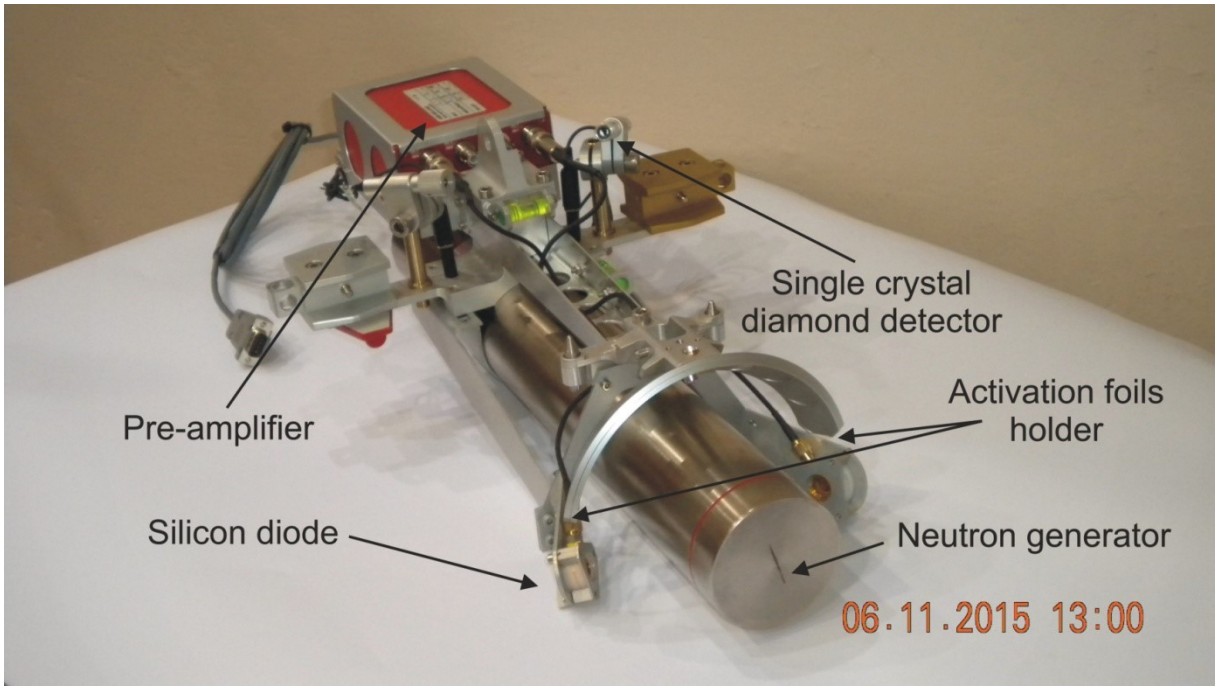

Fig. 2 *Neutron Generator with the mechanical support needed for remote handling gripping during the JET in vessel calibration, and to support the "monitoring detectors" and pre-amplifier (first NPL campaign).*

3. Activation measurements and analyses

3.1 Neutron activation reactions and their products

The activation reactions chosen for the monitoring foils were selected based on numerous requirements. Specifically, the cross section for the reaction products needed to be relatively large and well known. Also, the reaction thresholds should be sufficiently high in order to discriminate lower energy neutron scatter. The reaction products should emit gamma radiation that can be clearly measured using gamma spectrometry methods. The latter requirement mainly limits isotope selection to those of sufficiently long half-life and large branching intensities of the emitted photons to be useful for immediate post irradiation measurements. The reaction cross sections must also be from one of the standard Fusion dosimetry libraries. Finally, the nuclear reactions chosen for NG characterization should also parallel the foil reactions to be used during the DTE2 campaign in the JET KN2 diagnostic.

Several neutron-induced nuclear reactions were considered during the selection process for NS characterization. Given the above requirements, the following nuclear reactions were selected as activation monitors for 14.1 MeV neutrons: $^{27}Al(n,p)^{27}Mg$, $^{56}Fe(n,p)^{56}Mn$, $^{27}Al(n,\alpha)^{24}Na$, and $^{93}Nb(n,2n)^{92m}Nb$. It should also be noted that any interactions of high energy neutrons with the NG component materials slow the neutrons down and broaden their low-energy spectrum. Furthermore, the NG emits not only (d,t) neutrons but also trace amounts of neutrons from (d,d) and (t,t) reactions. Thus, detection of low-energy neutrons was necessary and they were monitored with the $^{115}In(n,n')^{115m}In$ nuclear reaction. Finally, note that the niobium foil reaction, $^{93}Nb(n,\alpha)^{90}Y$, leads to α-particle emission, which will not be incorporated into the yield calculations due to the relatively low production rate.

Nuclear data for analysis was taken from the International Reactor Dosimetry and Fusion File (IRDFF, volume 1.05) [8]. Except for $^{93}Nb(n,\alpha)^{90}Y$, which was not listed in the IRDFF-1.05 and was therefore taken from the TALYS-based Evaluated Nuclear Data Library (TENDL, volume 2014 [9]) instead. Fundamental Nuclear data parameters relating to the products of nuclear reactions, the gamma lines, intensities and half-lives were taken from the National Nuclear Data Center, Brookhaven National Laboratory, USA.

The cross sections for the above-mentioned reactions are plotted in fig 3. The main parameters for the radioactive products of selected nuclear reactions are listed in the table 1.

Table 1. *Main parameters of nuclear reaction products.*

Product of reaction	Half life	Energy of the most intense gamma lines [keV]	Intensity
$^{27}Al(n,p)^{27}Mg$	9.46 min	843.8	0.72
$^{56}Fe(n,p)^{56}Mn$	2.58 h	846.7	0.99
$^{27}Al(n,\alpha)^{24}Na$	14.99 h	1368.6	0.99
$^{93}Nb(n,2n)^{92m}Nb$	10.25 day	934.4	0.99
$^{93}Nb(n,\alpha)^{90}Y$	3.19 h	202.5	0.97
$^{115}In(n,n')^{115m}In$	4.49 h	336.2	0.46

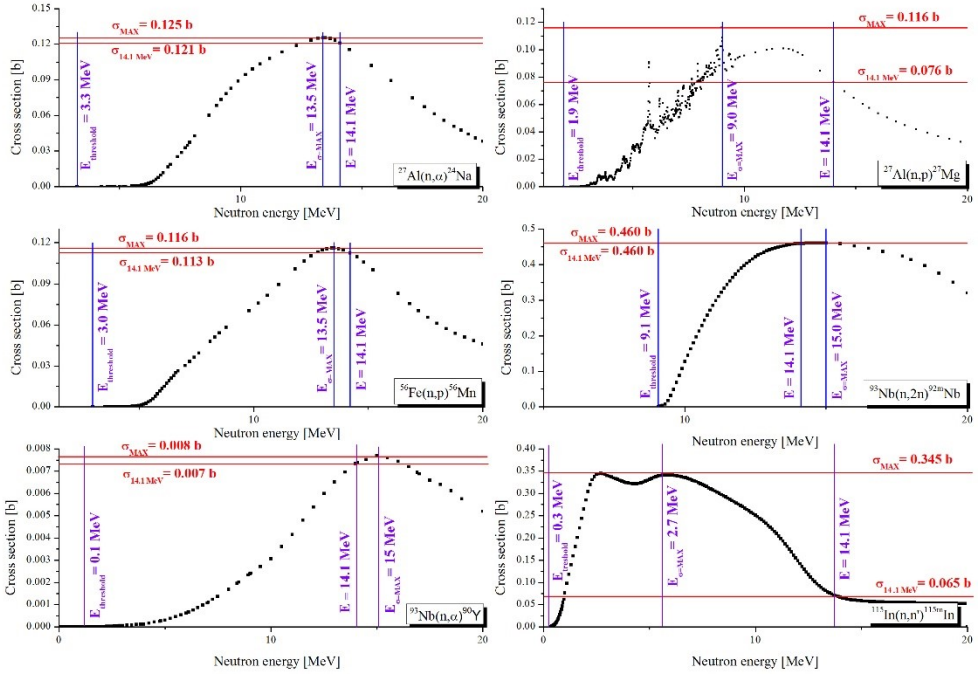

Fig. 3 *Cross sections for the selected nuclear reactions. $E_{threshold}$ and $E_{\sigma=MAX}$ are the neutron energy threshold and the energy where the cross section has a maximum, respectively; σ_{MAX} and $\sigma_{14.1\ MeV}$ are the maximum value of the cross section and the value of the cross section at 14-MeV, respectively. The $^{93}Nb(n,\alpha)^{90}Y$ data is taken from the TENDL 2014 library. The remainder of the data is taken from the IRDFF v. 1.05 library.*

3. 2 Neutron emission rate calculation

The neutron-induced radioactivity in a sample material can be expressed as:

$$A=Y_n \cdot R \cdot N_T\,(1-\exp(-\lambda \cdot t_A)) \qquad (1)$$

$$N_T=(m \cdot f \cdot A_v)/w \qquad (2)$$

$$R=\int_0^{\infty}\varphi(E)\cdot\sigma(E)dE=\langle\varphi(E)\cdot\sigma(E)\rangle \qquad (3)$$

where: Y_n is the neutron yield [n·s^{-1}], A is the activity of a particular isotope induced by neutron activation [Bq], R is the reaction rate [reaction·s^{-1}], m is the mass of activated sample [g], f is the abundance of target nuclei in the sample [unitless], A_v is Avogadro's constant [mol^{-1}], w is the atomic mass of the target nucleus [g·mol^{-1}], λ is the decay constant of the activation product, t_A is the activation time, $\varphi(E)$ is the distribution of neutrons as function of energy, and $\sigma(E)$ is the reaction cross section [b].

The radioactivity of i-th activations ($t_{Ai} \neq t_{Ai+1}$) and the subsequent cooling time ($t_{Ci} \neq t_{Ci-1}$) can be expressed as:

$$A_n = Y_n / t \cdot N_T \cdot \langle\varphi(E)\cdot\sigma(E)\rangle \cdot \sum_i B_i\left(1-\exp(-\lambda \cdot t_{Ai})\right)\cdot\exp(-\lambda \cdot t_{Ci}) \qquad (4)$$

where t is the total irradiation time, B_i is a normalization factor which takes into account changes in the neutron yield, recorded by the monitoring SDD during successive NG pulses of duration t_{Ai}. Note that in the case of a single NG pulse, eq. (4) simplifies to eq. (1).

3.3 Monte Carlo N-Particle calculation of the neutron spectra

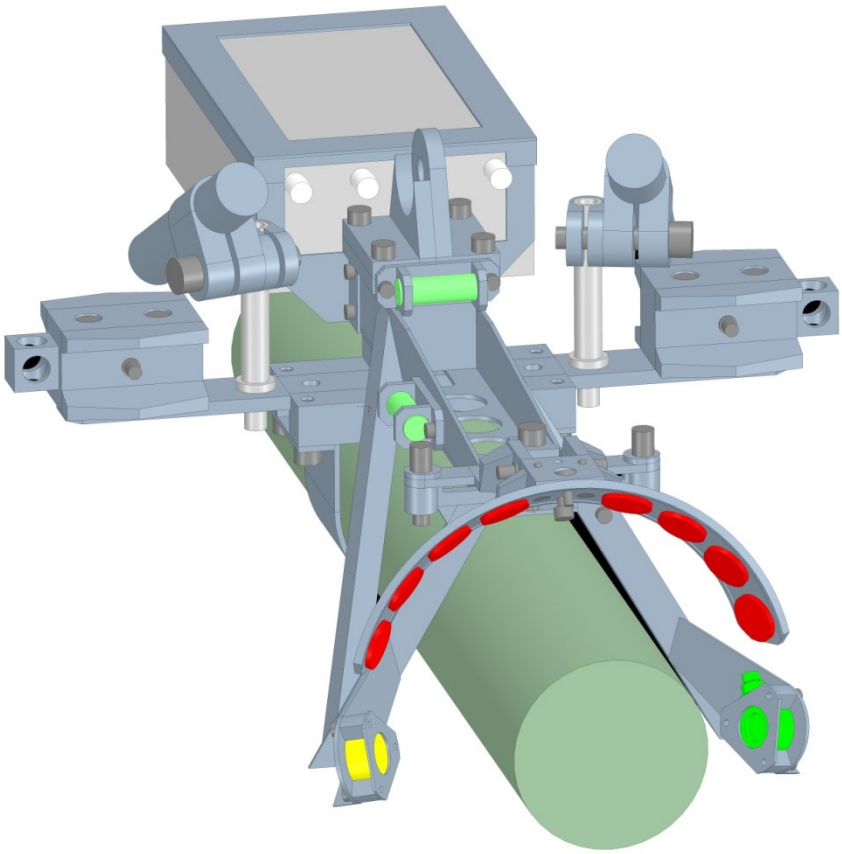

Fig. 4 *MCNP model of the neutron generator (dark green) and holder (grey) with attached foils (red coins).*

A simplified CAD version of the NG, activation foils, monitoring detectors and attachments was created and converted to a Monte Carlo N-Particle Transport Code (MCNP) compatible geometry using the SuperMC/MCAM code [10,11] (see fig. 4). Neutron transport calculations, using MCNP, were performed to derive reaction rates in the activation foils being used. The neutron emission spectrum, used in the source routine, consisted of a weighted sum of expected source components corresponding to (d,t) and (t,d) reactions at different incident ion beam energies. Spectra of these source components were obtained through simulations using a custom source subroutine [12] implemented in MCNP. The weighting factors for different source components in the source description were determined by SDD spectral measurements during the first NPL campaign.

The results of the MCNP calculations of neutron energy distributions at the positions occupied by the activation foils can be seen in fig. 5. The neutrons with energies below 13 MeV are the result of scattering of source neutrons through the NG body.

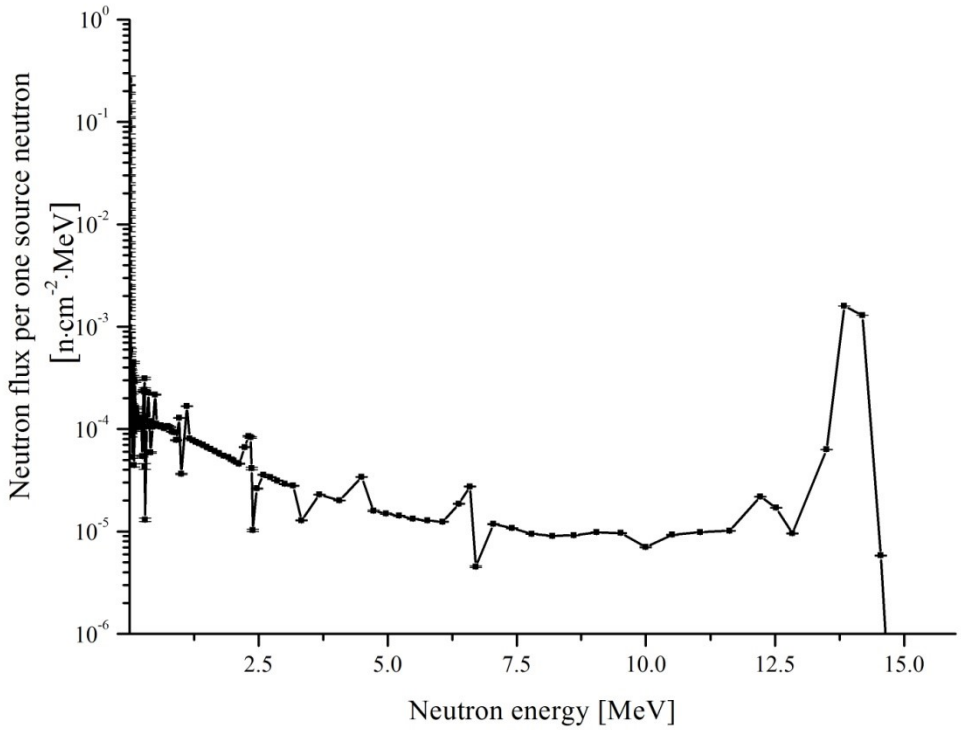

Fig. 5 *The MCNP calculated neutron spectrum at the activation foil position.*

3.3 Gamma-ray spectrometry

A high purity germanium (HPGe, Canberra) detector was used for the gamma-ray spectrometry measurements. The detector had a relative efficiency of approximately 30 % for 1332-keV photons with a resolution 1.8-keV. It was supplied with Canberra Laboratory Sourceless Calibration Software (LabSOCS) and numerical characterisation, which allows for source-less energy-efficiency calibration. All the activation foils used for the NPL measurement campaigns were of 18-mm diameter and 1-mm thickness, except for niobium foils which were 2-mm thick. Four aluminium, four iron, and four niobium foils were mounted on the holder, activated and subsequently measured sequentially. The gamma-ray measurements were conducted in two geometries. The "cylindrical" geometry consisted of a circular plexiglass holder with a hole at its centre. The holder was mounted on the detector endcap and the stack of foils was placed in the hole. The "rosette" geometry consisted of an aluminium holder mounted on the detector end cap. A square indent was drilled in the plate so that the four activation samples could be placed at opposing ends of the geometry. The efficiency of detecting a gamma-ray in HPGe detectors depends on the photon energy, the sample size, and the measurement geometry. Thus, for each foil set, the energy-efficiency calibration was calculated using LabSOCS. The option of measuring in two geometries enables the selection of the maximum efficiency for the chosen gamma line being measured. The following uncertainties, for the various photon energies measured, are assigned for the efficiency calibration: 7 % standard deviation (SD) for photons of less than 150 keV in energy, 6 % SD for photons between 150–400 keV, and 4.3 % SD for photons between 400–7000 keV [13]. These are standard LabSOCS figures, while in our studies using Marinelli sample geometries, an efficiency uncertainty of 0.1 % was observed [14]. On the

other hand, values of detection efficiency uncertainty rapidly increase with changing samples density. Based on the cross calibration of the above detector with point like source and measurements of metal samples activated during Neutron Source Calibration we deducted that the most reasonable efficiency uncertainty for photons between 400-7000 keV is 8 % [2].

All the aluminium foils were measured twice. One set of measurements was conducted 12 minutes after the irradiation had concluded. This 12 minute cooling time allowed for the decay of the short lived ^{28}Al, from the ^{27}Al(n,γ)^{28}Al activation reaction. Then 40 minutes of measurement in the cylindrical geometry allowed for the recording of the ^{27}Mg activity. The iron sample was then measured for 30 min with a cylindrical geometry to determine the activity of ^{56}Mn present. The aluminium samples were then measured a second time in the rosette geometry for 900 min and the activity of ^{24}Na was determined. Finally, ^{92m}Nb metastable was measured in the four samples for 420 minutes in the rosette geometry. The presence of the ^{90}Y radionuclide was also detected in the niobium sample, as unexpected. The low energy neutron monitoring foil, indium, was allowed to cool for 4 h before it's measurement, which allowed it to partly decay to ^{116}In and to decrease the Compton background around 336.2-keV peak of full energy absorption being measured.

4. Results

The normalized amplitudes of the neutron yield, for NG1 and NG2 are presented in fig. 6 and 7, as a result of the signal (counts per second) from the monitoring SDD. The shot numbers are presented on the horizontal axis. The irradiation duration was typically 1200 s; however, there were also shots with durations of 900 s and 600 s. The variations in Y_n amplitudes, measured with the SDD, were taken into account when deriving the B_i factors in eq. (4).

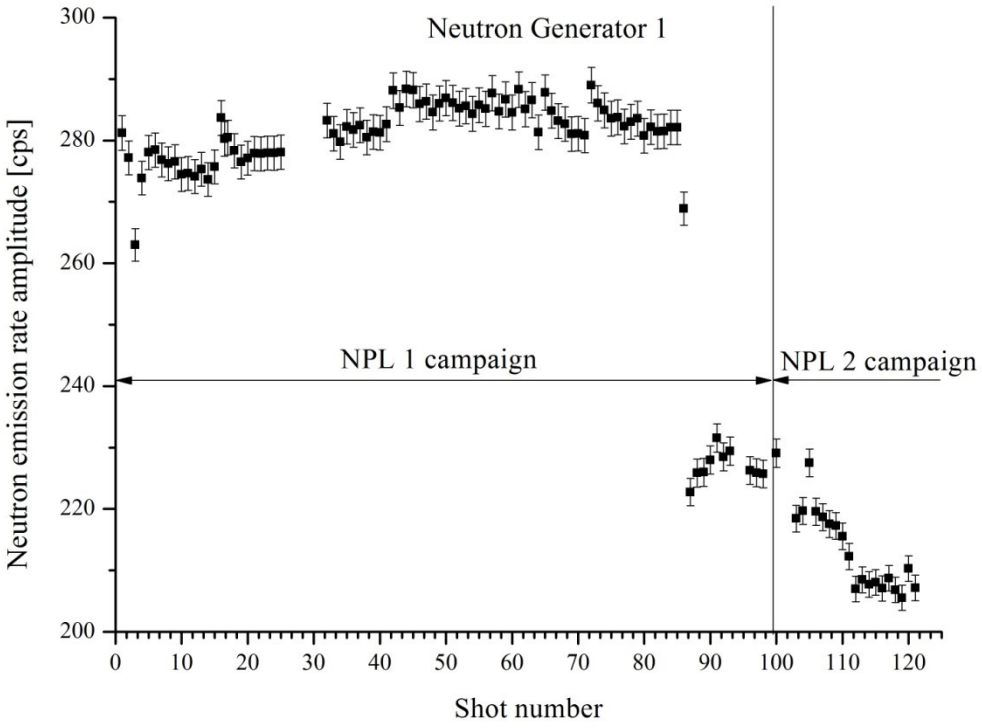

Fig. 6 *Relative amplitude of Y_n for NG1 based on SDD measurements.*

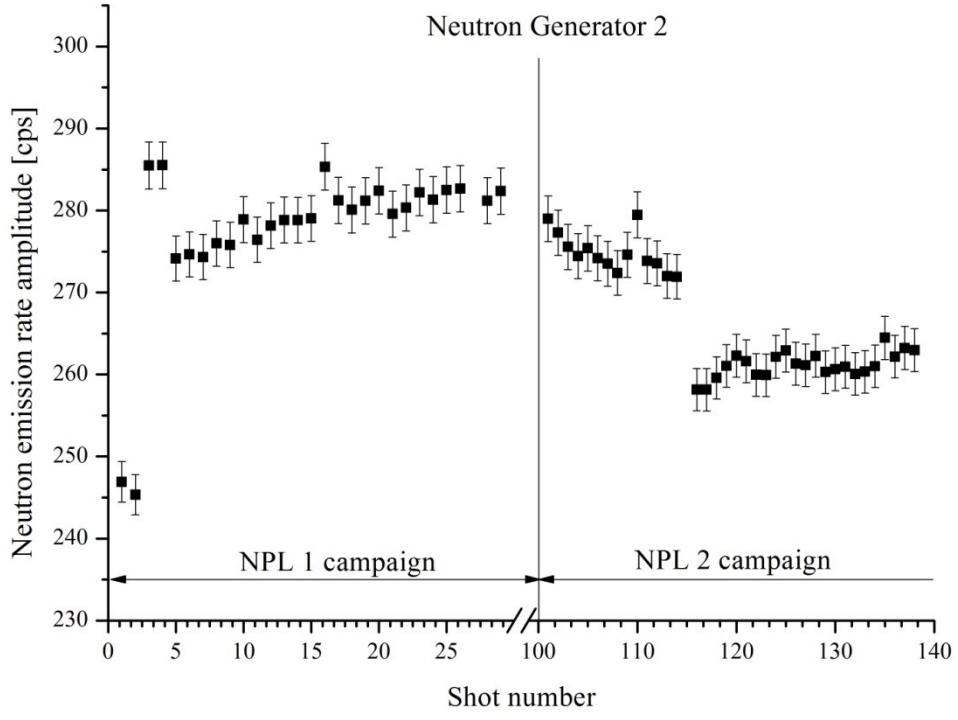

Fig. 7 *Relative amplitude of Y_n for NG2 based on SDD measurements.*

The measured gamma-ray spectrum of the aluminum sample displayed the characteristic peaks of ^{27}Mg and ^{24}Na, whilst the standard iron sample showed full energy peaks resulting from the decay of ^{56}Mn. The niobium was therefore identified as the most effective neutron monitor for the DTE2 experimental campaign. The decay gamma spectrum of the activated niobium, during the fourth day of the NPL campaign which is presented in fig. 8.

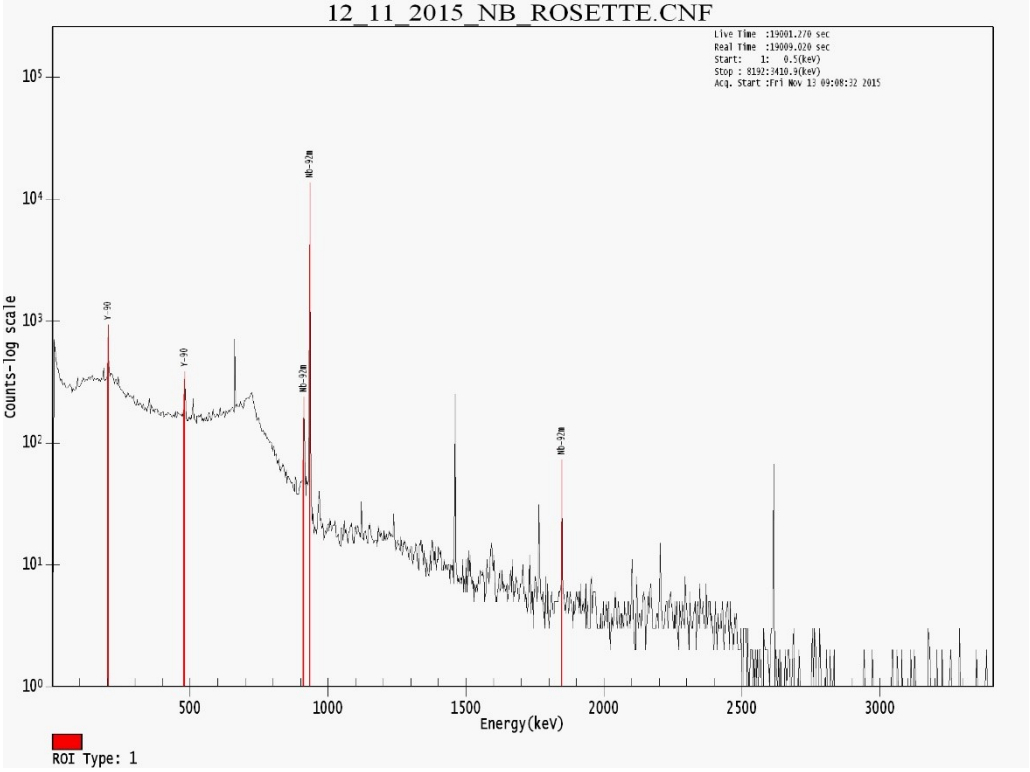

Fig. 8 *Gamma-ray spectrum (original screenshot from Genie2000) of niobium activation foil irradiated on Nov 10th and measured the following day. In addition to ^{92m}Nb and the natural background radionuclide peaks observed, two full energy absorption peaks for ^{90}Y are visible (from left: two red peaks from ^{90}Y, three red peaks from ^{92m}Nb).*

As mentioned above, the ^{90}Y radionuclide from the (n,α) reaction was detected in the niobium sample, along with ^{92m}Nb. This is evidence of a highly efficient activation process.

Fig. 9 shows the build-up of ^{27}Mg, ^{56}Mn, ^{24}Na and ^{92m}Nb radioactivity on the second day of the experimental campaign and is representative of the build-up pattern observed throughout the campaigns. The graphs show the result of calculations that took into account the observed variations in neutron yield, irradiation times and cooling times for each pulse. For ^{27}Mg, the accumulated activity oscillates around a specific level with little variation due to its short half-life relative to the irradiation and cooling times. Saturated activity was not reached here. For the other radionuclides, the activity build-up is essentially linear due to their long half-lives relative to the irradiation and cooling times.

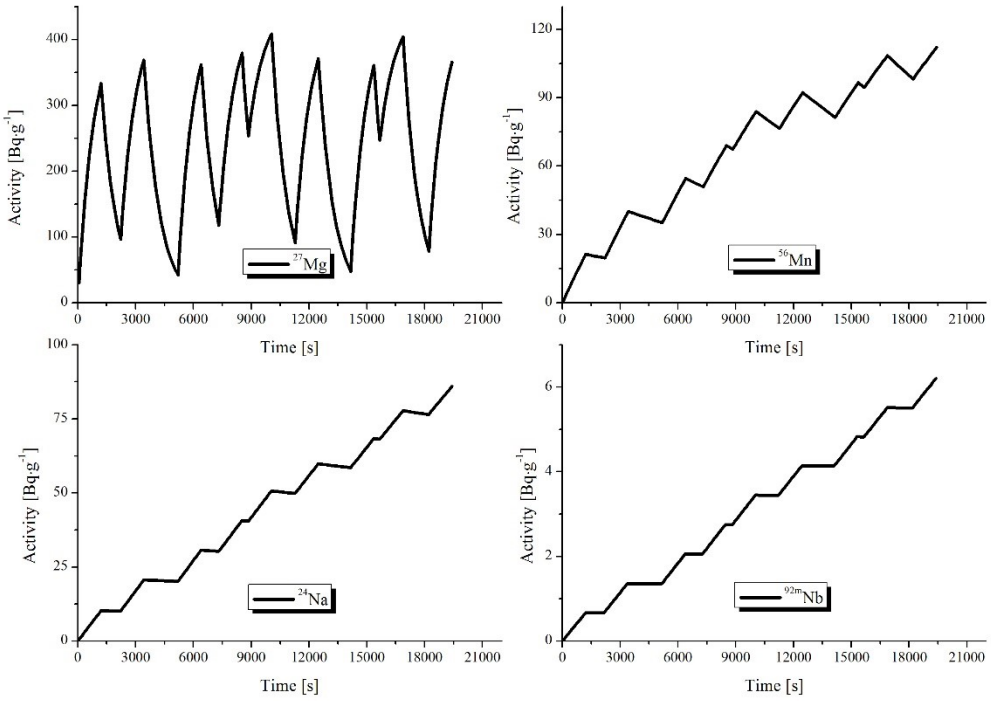

Fig. 9 *Time evolution of radioactivity for particular reaction products during the second day of irradiation under real conditions*.

Over both NPL experimental campaigns, the measured ^{27}Mg radioactivity, after a single day's irradiation, was in the range of 243–409 Bq·g^{-1}. The ^{24}Na radionuclide was measured twice with identical results; however, the uncertainty in the measured activity was lower for the longer measurement. The ^{24}Na radioactivity was in the range of 22–86 Bq·g^{-1}. For ^{56}Mn formed during the irradiation of the iron sample, the measured radioactivity was in the range of 44–126 Bq·g^{-1}. The results for ^{92m}Nb varied over the range of 1.44–6.35 Bq·g^{-1}. During the last day of the first experimental campaign at NPL, indium foils were used instead of aluminium foils. The radioactivity of ^{115m}In was 42 Bq·g^{-1}.

The estimated neutron emission rate was based on an MCNP-calculated neutron reaction rates at the foil locations and on the measured radioactivity as given by eq.4, fig. 9 and 10, show plots of the estimated neutron emission rates for particular reaction products for each day of the experimental campaigns. The calculated reaction rates per one source neutron were $8.34 \cdot 10^{-5}$ for ^{27}Al(n,p)^{27}Mg, $1.15 \cdot 10^{-4}$ for ^{56}Fe(n,p)^{56}Mn, $1.24 \cdot 10^{-4}$ for ^{27}Al(n,α)^{24}Na, and $4.45 \cdot 10^{-4}$ for ^{93}Nb(n,2n)^{92m}Nb. Fig. 9 showing NG1, and fig. 10 showing NG2.

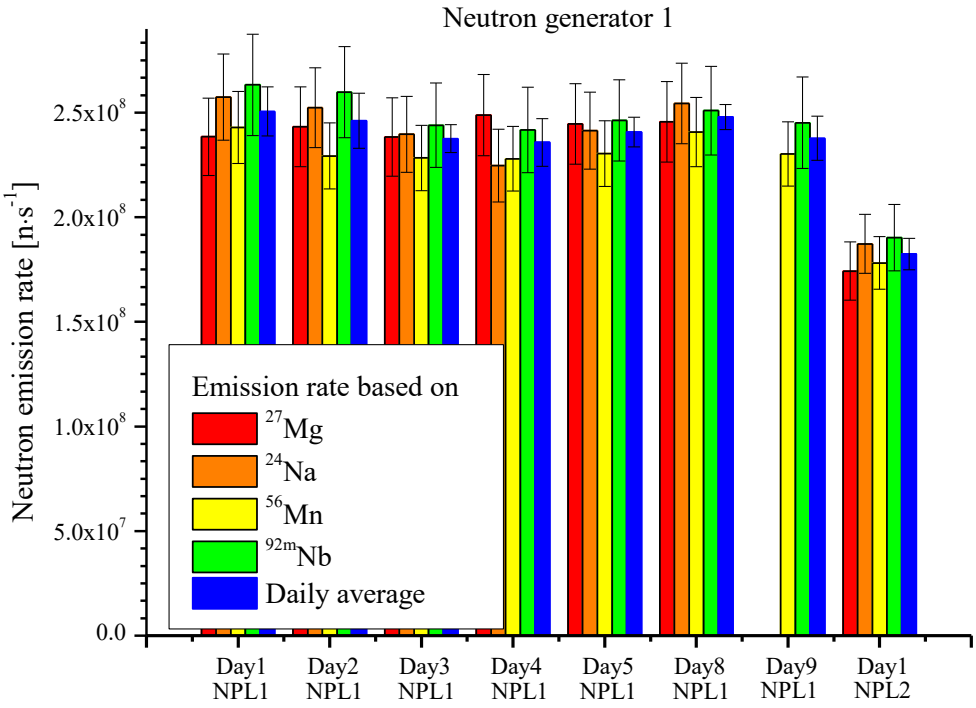

294

295 ***Fig. 10*** *Estimated neutron emission rates for NG1 based on MCNP-calculated neutron spectra for the foils. The*

296 *error bars represent the total uncertainty (1σ).*

297

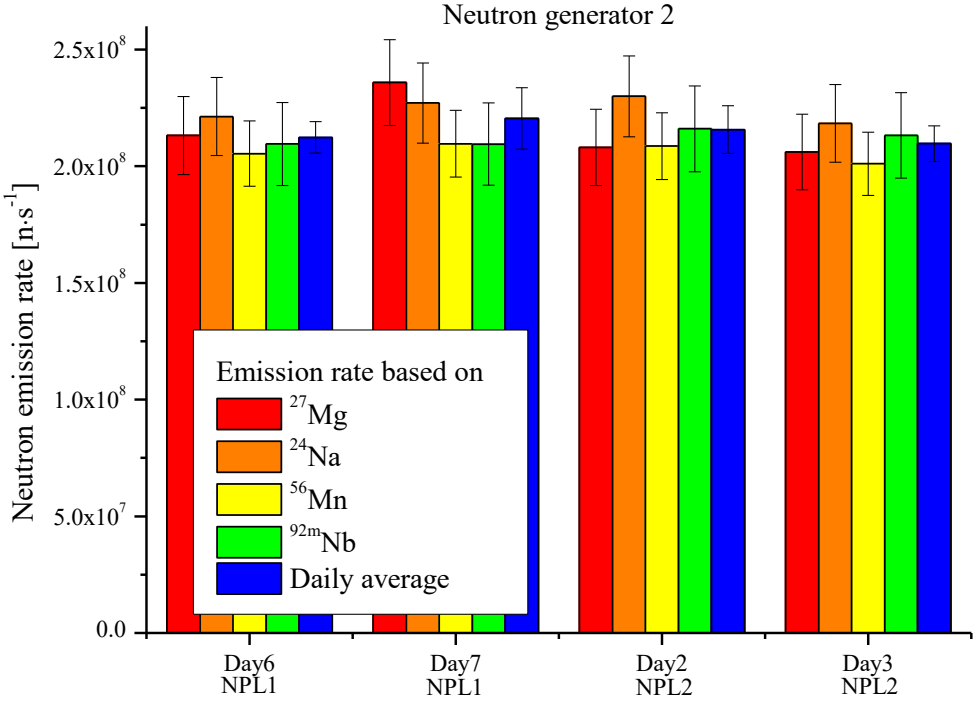

298

Fig. 11 *Estimated neutron emission rates for NG2 based on MCNP-calculated neutron reaction rates for the foils. The error bars represent the total uncertainty (1σ).*

The total uncertainty in the neutron emission rate was calculated as the quadratic sum of different contributions, including:

- The statistical uncertainty in the activity, the branching ratio, and the computed decay correction factor. This uncertainty amounts to 8.3% for ^{27}Mg, 8.1% for ^{24}Na, 7.5% for ^{56}Mn and 8.9% for ^{92m}Nb.
- The uncertainty in the number of target nuclei, which is directly related to the precision of the sample mass measurement, which is equal to 0.01 g for the foil samples used here. This uncertainty amounts to 0.39% for Al samples, 0.12% for Fe samples and 0.06% for Nb samples.
- The uncertainty of the sums in eq. 4 was estimated to be Mg: 1.51%, Na: 1.16%, Mn: 1.16%, Nb: 1.16%, because all components in this part of the equation were correlated to each other. The highest uncertainty was for magnesium sample due to its short half-life.
- The uncertainty on the reaction rates calculated by MCNP is less than 0.1%. The uncertainties of cross sections in the activation calculation were not taken into account.

The resulting total uncertainty of the neutron emission rate based on singular nuclear reaction is in the range 6.7-9.2%. The discrepancies between the reactions on the same day have been observed, outside the combined uncertainties of the measurements. The SD for the daily average neutron emission rates for NG1 was within the range of 2.5-4.9 %, with the exception of day 2 of the NPL 1 campaign, where it was greater than 5 %. For NG2 the SD was in the range of 3.2-6.0 %, where more than 5 % was observed only on the seventh day of the NPL 1 campaign. It should be noted that when the ion beam current intensity changes, the neutron emission rate is affected. The monitoring foils are distributed approximately 180 degrees, asymmetrically across the main axis of the NG. Deviations of the ion beam in the radial direction result in neutron emissions that are no longer symmetric about the centre of the NG target. Which can result in variations in the measured neutron fluence at the foil positions.

The neutron yields measured by the activation foils were compared with the signals obtained by the calibrated monitoring SDD, on a day to day basis, and they were found to agree in all cases within 8%.

5. Conclusions

A 14.1 MeV neutron generator was selected as the NS for the forthcoming in-vessel calibration of neutron diagnostics on the JET tokamak in preparation for DT operations. After detailed analysis of the nuclear reaction parameters. the following reactions were selected for the purpose of measurements: ^{27}Al(n,p)^{27}Mg, ^{56}Fe(n,p)^{56}Mn, ^{27}Al(n,α)^{24}Na, ^{93}Nb(n,2n)^{92m}Nb. Two NGs have been characterized in terms of neutron emission (rate) and angular distributions at the National Physical Laboratory. The activation technique has been used to measure the NGs neutron emission rates. The same methodology will be used as a complementary technique for NG neutron yield monitoring during the in vessel process. Throughout the NPL campaigns', the activity of the reaction products has been measured using gamma-ray spectrometry with less than 10 % uncertainty. The exception was the measurements with ^{115}In. due to the larger uncertainty in determining the detector efficiency at lower energies. The NG emission rates have been derived using MCNP-calculated reaction rates. The

uncertainty for these values was in the range 6.7-9.2 %. The SD for the daily average neutron emission rate for NG1 was greater than 5 % on a solitary occasion; this was on the second day of the NPL 1 campaign. The NG2 SD was more than 5 % only once, on the seventh day of the NPL 1 campaign. The neutron yields measured by the activation foils were in agreement within 8% with the yields obtained by the calibrated monitoring SDD.

Acknowledgments

"This work has been carried out within the framework of the EUROfusion Consortium and has received funding from the Euratom research and training programme 2014-2018 under grant agreement No 633053. The views and opinions expressed herein do not necessarily reflect those of the European Commission."

References

[1] X-5 Monte Carlo Team, MCNP - A General N-Particle Transport Code, Version 5., Los Alamos National Laboratory, 2003.

[2] D.B. Syme, S. Popovichev, S. Conroy, I. Lengar, L. Snoj, C. Sowden, L. Giacomelli, G. Hermon, P. Allan, P. Macheta, D. Plummer, J. Stephens, P. Batistoni, R. Prokopowicz, S. Jednorog, M.R. Abhangi, R. Makwana, JET EFDA contributors, Fusion Yield measurements on JET and their Calibration, Fusion Eng. Des. 89 (2014) 2766–2775. doi:10.1016/j.fusengdes.2014.07.019.

[3] P. Batistoni, 15.5 Nuclear fusion technology in conjunction with DT operations at JET in support of ITER, in: 29th Symp. Fusion Technol., Prague, 2016: p. 17.

[4] E.P. Bogolubov, V.I. Ryzhkov, D.I. Yurkov, VNIIA research, engineering, and manufacturing capabilities to develop neutron generators and equipment on their basis, in: Int. Sci. Tech. Conf. Portable Neutron Gener. Technol. Their Basis, Moscow, 2012: pp. 22-26.

[5] http://www.vniia.ru/ (accessed November 21,2016).

[6] A. Klix, M. Angelone, P. Batistoni, A. Cufar, Z. Ghani, L. Giacomelli, S. Jednorog, E. Laszynska, I. Lengar, S. Lorenti, A. Milocco, L.W. Packer, M. Pillon, S. Popovichev, M. Rebai, S.D. Rigamonti, H. Roberts, L. Snoj, E. Tardocchi, D. Thomas, P1.066 Characterization of a neutron generator for the JET monitoring system calibration with NE-213 spectrometer, in: 29th Symp. Fusion Technol., Prague, 2016: p. 137.

[7] E. Laszynska, S. Jednorog, A. Ziolkowski, M. Gierlik, J. Rzadkiewicz, Determination of the emission rate for the 14 MeV neutron generator with the use of radio-yttrium, Nukleonika. 60 (2015) 319-322. doi: 10.1515/nuka-2015-0040.

[8] R. Capote, K.I. Zolotarev, V.G. Pronyaev, A. Trkov, E.M. Zsolnay, H. K. Nolthenius, (2014, October). International Reactor Dosimetry and Fusion File IRDFF v.1.05, (2012). https://www-nds.iaea.org/IRDFF/ (accessed June 10, 2016).

[9] A. J. Koning, D. Rochman, S.C. van der Marck, J. Kopecky, J.Ch. Sublet, S. Pomp, H. Sjostrand, R. Forrest, E. Bauge, H. Henriksson, O. Cabellos, S. Goriely, J. Leppanen, H. Leeb, A. Plompen, R. Mills, S. Hilaire, TENDL-2014:TALYS-based evaluated nuclear data library, (2015). ftp://ftp.nrg.eu/pub/www/talys/tendl2014 (accessed June 10, 2016).

[10] Y. Wu, FDS Team, CAD-based interface programs for fusion neutron transport simulation, Fusion Eng. Des., 84 (2009) 1987-1992. doi:10.1016/j.fusengdes.2008.12.041.

[11] Y. Wu, J. Song, H. Zheng, G. Sun, L. Hao, P. Long, L. Hu, FDS Team, CAD-Based Monte Carlo Program for Integrated Simulation of Nuclear System SuperMC, Ann. Nucl. Energy., 82 (2015) 161-168. doi:10.1016/j.anucene.2014.08.058.

[12] A. Milocco, A. Trkov, M. Pillon, A Monte Carlo model for low energy D–D neutron generators, Nucl. Instruments Methods Phys. Res. Sect. B Beam Interact. With Mater. Atoms. 271 (2012) 6-12. doi:10.1016/j.nimb.2011.10.009.

[13] F. L. Bronson, Validation of the accuracy of the LabSOCS software for mathematical efficiency calibration of Ge detectors for typical laboratory samples, Radioanal. Nucl. Chem. 255 (2003) 137–141. doi:10.1023/A:1022248318741.

[14] S. Jednorog, A. Szydlowski, M. Scholz, M. Paduch, B. Bienkowska, Preliminary determination of angular distribution of neutrons emitted from PF-1000 facility by indium activation, Nukleonika. 57 (2012) 563–568.